PRECIPITATION AND ROOM TEMPERATURE DEFORMATION BEHAVIOUR OF INCONEL 718

M. Sundararaman, P. Mukhopadhyay and S. Banerjee

Metallurgy Division
Bhabha Atomic Research Centre
Bombay 400 085, India

Abstract

Some aspects of the precipitation of intermetallic phases (the metastable $\gamma'(L1_2$ structure), the metastable $\gamma''(DO_{22}$ structure) and the equilibrium δ (DO_a structure) phases) including the sequence of their precipitation, in the commercial, nickel–iron based superalloy, Inconel* 718, have been studied over a wide range of ageing temperatures. At certain ageing temperatures, the frequent occurrence of physical association between γ' and γ'' precipitates, giving rise to a variety of composite precipitate morphologies, has been observed. The δ phase, which, is the equilibrium intermetallic phase occurring in Inconel 718, has been found to nucleate at the geometric stacking faults within the pre–existing γ'' precipitates at temperatures below about 1173 K on prolonged ageing. At higher ageing temperatures δ phase precipitation occurs directly in the austenite matrix. These observations have been rationalised in terms of the relative concentrations of solute elements participating in the formation of the precipitating phases and also in terms of the free electron concentration model.

A study of the room temperature deformation behaviour of the aged alloy has revealed the operation of a novel precipitate shearing mechanism. When the γ'' particle size exceeds a critical value (about 10 nm), these particles are sheared by the passage of true crystallographic deformation twins which do not disrupt the ordered atomic arrangements within the precipitates. When the particle size is smaller than this critical value, precipitate shearing occurs by the movement of groups of dislocations which restore complete order within all the three γ'' variants after their passage. Strengthening due to the presence of γ'' precipitates has been estimated as a function of precipitate size, corresponding to different particle shearing and bypassing mechanisms and the estimated values have been compared with the experimental data. The stability of the deformation microstructure has been studied as a function of temperature in the range of 923 K to 1073 K.

* Inconel is a trademark of Inco Alloys International, Inc., Huntington, WV

Superalloys 718, 625, 706 and Various Derivatives
Edited by E.A. Loria
The Minerals, Metals & Materials Society, 1994

Introduction

Although most of the precipitation hardenable commercial, nickel base superalloys are strengthened primarily by precipitates of the γ' phase, some alloys (such as Inconel 718) have been developed in which the major contribution to precipitation hardening is derived from the γ" phase [1–3]. The precipitation of intermetallic phases in Inconel 718 has been extensively studied and it has been found that the major intermetallic phases that precipitate in the austenite (γ) matrix in this alloy are the metastable γ" (DO_{22} structure) and γ' ($L1_2$ structure) phases and the equilibrium δ (DO_a structure) phase [3–9]. All the three phases are of the A_3B type: the γ" and the δ phases are based on the composition Ni_3Nb and the γ' phase on Ni_3(Al,Ti). Age hardening in this alloy is brought about mainly by the homogeneously nucleated γ" precipitates, which are coherent, disc shaped particles with $\{100\}_\gamma$ habit and bear the orientation relationship $\{100\}_{\gamma"} // \{100\}_\gamma$; $[001]_{\gamma"} // <001>_\gamma$ with the austenite matrix. Some strengthening is also brought about by the γ' precipitates which bear a cube–to–cube orientation relationship with the matrix and have a spheroidal/cuboidal morphology [3,10]. The equilibrium δ phase, which can form in this alloy during processing or during service [1], generally appears in the form of plate shaped precipitates, though a globular morphology has also been occasionally observed. Controlled precipitation of the δ phase at the grain boundaries is believed to have a beneficial effect on stress rupture ductility [11]. In addition to these intermetallic phases, primary and secondary carbide precipitates (MC and $M_{23}C_6$ types) also occur in this alloy [12–14]. However, this aspect will not be discussed here since the emphasis in the present paper is not on carbide precipitation.

One of the issues addressed in this paper is the sequence of precipitation of the metastable intermetallic phases: whether the γ' and the γ" phases form simultaneously or in a sequential manner and whether these two precipitate types nucleate independently of one another or whether the precipitation of one type facilitates the precipitation of the other. Cozar and Pineau [15] have observed that in Inconel 718 type alloys a physical association between γ' and γ" particles often results in the evolution of a "compact morphology" in which cuboidal γ' particles are coated on all the six faces with the γ" phase. This happens when the alloy composition is so adjusted that the ratio of the combined aluminium and titanium content to that of the niobium content exceeds about 0.9. The coarsening kinetics of the composite precipitates exhibiting the "compact morphology" is very sluggish. Thus their formation enhances the microstructural stability of the alloy. Although the aforementioned ratio is much smaller than 0.9 in Inconel 718 itself, a physical association between γ' and γ" particles has been observed in this alloy also in a recent investigation [9]. The relevant observations will be summarised here.

Deformation mechanisms and deformation microstructures pertaining to Inconel 718 type alloys have been studied in detail [4,10,16]. Some investigators are of the view that deformation occurs in bands rather than by coplanar flow of dislocations and that faults are produced within the γ" particles along the slip planes during deformation [4]. Some others, however, have suggested that deformation occurs mainly by the motion of doublets of unit dislocations [16]. The present authors have studied the evolution of the deformation microstructure in this alloy at room temperature as a function of the γ" particle size and have found that when this size exceeds a critical value, precipitate shearing occurs by deformation twinning of the precipitates [17]. This mode of dislocation – precipitate interaction with reference to the room temperature deformation behaviour of Inconel 718 is another topic discussed in this paper. The dependence of the thermal stability of the deformation microstructure on the ageing temperature has also been briefly described. The observations have been explained on the basis of a mechanism of the γ"–δ transformation.

Table I Chemical Composition of Inconel 718 Alloy

Element	Ni	Cr	Fe	Nb	Mo	Al	Ti	Mn	Si	C
Conc. (wt.%)	52.67	18.37	18.06	6.00	2.91	1.00	0.45	0.21	0.29	0.04
Conc. (at.%)	51.78	20.39	18.66	3.73	1.75	2.14	0.54	0.22	0.60	0.19

Conc.– Concentration; wt.% – weight percent, at.% – Atomic percent.

Some aspects of the crystallography of DO_{22} and DO_a Structures

The body centred tetragonal DO_{22} unit cell of the γ"– Ni_3Nb phase, as illustrated in Fig. 1 (a), can be regarded as a stacking of two face centred cubic (A1) unit cells one upon the other, with niobium atoms occupying the corners and the body centre of the resulting tetragonal cell. Since the axial ratio is very close to two for γ" and the disordered structure of DO_{22} is A1, all structural descriptions in this paper will be presented in terms of fcc notations. The arrangement of atoms in the close packed (111) plane of a DO_{22} crystal [(112) plane in terms of DO_{22} Miller indices], whose tetragonal axis is parallel to the [001], direction is shown in Fig. 1(b). The stacking of six such atomic layers of Ni_3Nb stoichiometry, one above the other, in such a way that each layer is displaced with respect to the preceding one by a 1/3 $[1\bar{2}1]$ or a 1/3 $[\bar{2}11]$ vector, produces the DO_{22} structure. This stacking sequence can be described as $A_1B_1C_1A_2B_2C_2A_1$ .....

The orthorhombic DO_a unit cell associated with the δ–Ni_3Nb phase is illustrated in Fig. 2(a). The close packed plane in this structure is the (010) plane. The atomic arrangement in this plane (Fig. 2(b)) shows a rectangular arrangement of the minority (niobium) atoms, identical to that obtained in the close packed (111) plane of the DO_{22} structure (Fig. 1(b)). However, unlike in the latter structure, an ABABAB...type two–layer stacking sequence is encountered in the former structure. Algebraic expressions for the structure factor for different reflections in the DO_a and DO_{22} structures have been reported elsewhere [7,9].

It could be seen from Fig. 1(b) that while the lattice translation vector 2.1/2 $[\bar{1}10]$ maintains perfect order in the DO_{22} phase in the $[\bar{1}10]$ direction, displacements of 4. 1/2 $[\bar{1}01]$ and 4.1/2 $[0\bar{1}1]$ respectively are required to maintain perfect order along the $[\bar{1}01]$ and the $[0\bar{1}1]$ directions, where 1/2 $<1\bar{1}0>$ represent perfect translation vectors in the (111) plane of the disordered matrix. It may be mentioned in this context that Kirman and Warrington [4] or Chaturvedi and Han [10] have not noticed any evidence suggesting the involvement of the motion of quadruplets of unit dislocations in the deformation of Inconel 718. Oblak et al [16] on the other hand, have observed the presence of such four–dislocation groups in this alloy.

The passage of a single 1/6 $[11\bar{2}]$ partial dislocation on the (111) plane does not cause any change in the first nearest neighbour atoms but leads to the formation of a stacking fault. However, the movement of a 1/6 $[\bar{2}11]$ or a 1/6 $[1\bar{2}1]$ partial would produce a complex stacking fault and change the first nearest neighbour environment. The formation of such high energy complex stacking faults is quite unlikely. In the context of the γ" phase, partial dislocations with 1/6 $[11\bar{2}]$ Burgers vector play an important role in generating deformation twins as well as the equilibrium δ phase. The former can be produced by the passage of 1/6 $[11\bar{2}]$ partials on every (111) plane while the latter can be formed by the passage of these dislocations on every alternate (111) plane. This point will be discussed later. Dislocations

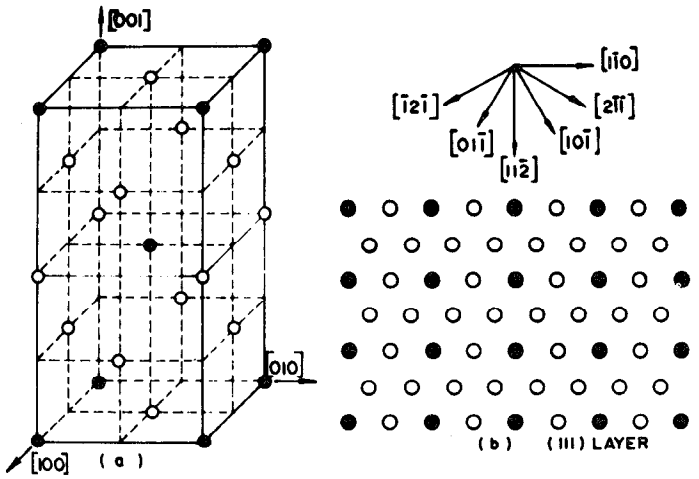

Fig. 1 – (a) Unit cell of DO_{22} (γ" –Ni_3Nb) structure and (b) Arrangement of atoms in the (111) plane of the DO_{22} structure. Nickel atoms are represented by open circles and niobium atoms by closed circles.

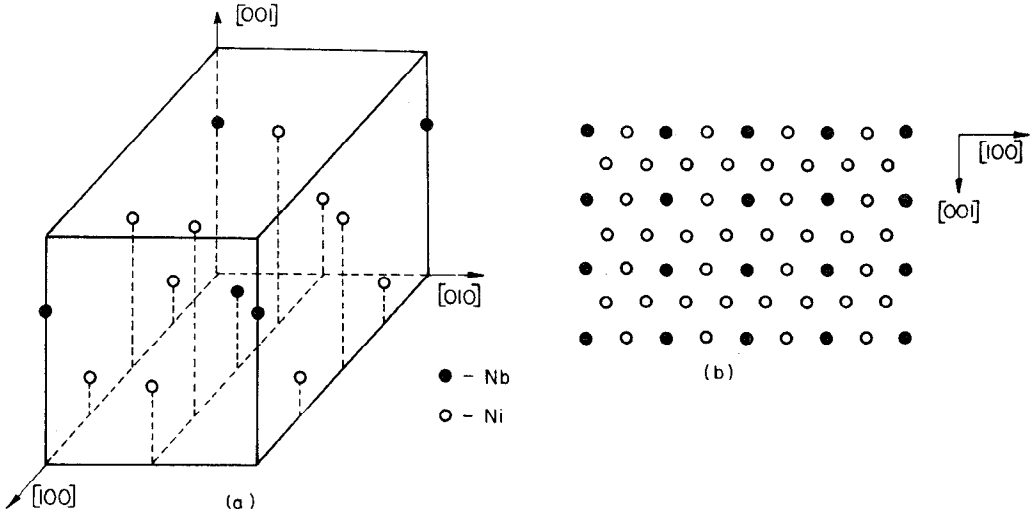

Fig. 2 – (a) Unit cell of DO_a (δ–Ni_3Nb) structure. (b) Atomic arrangement on the close packed (010) plane. This arrangement is similar to the atomic arrangement on the close packed plane of the DO_{22} structure in Fig. 1 (b).

with Burgers vectors other than those mentioned here have been considered in detail in an earlier publication and it has been shown that their occurrence is unlikely [17].

Experimental

Inconel 718 was obtained in the form of a 7 mm thick sheet. The chemical composition of the alloy is shown in Table I. The sheet was cold rolled down to 0.75 mm thickness. Specimens of suitable dimensions were obtained from the cold rolled material for transmission electron microscopy (TEM) and tensile testing. All samples were solution treated at 1373 K for 1 hour and then water quenched. Ageing of the solution treated samples was carried out for different periods of time in the temperature range of 923 K to 1223 K. The average γ'' particle size corresponding to any ageing treatment was determined from dark field micrographs obtained by imaging with {100} and {1 1/2 0} type superlattice reflections, with the foil oriented in a <001> orientation. Heat treated tensile specimens were deformed at room temperature in air in a floor model Instron machine, using a strain rate of $6.67 \times 10^{-4} s^{-1}$, to failure. Gauge portions of deformed samples were subjected to different ageing treatments in the temperature range of 923 K to 1073 K and processed for TEM studies with a view to examining the thermal stability of the deformation microstructure. The preparation of TEM specimens has been described elsewhere [9,17].

Results

The typical microstructure of the solution treated and quenched alloy is illustrated in Fig. 3. The austenite matrix was free from any intermetallic phase precipitates and contained some randomly distributed, blocky, primary carbide (niobium rich MC type) particles. It also contained a fairly high density of dislocations. These dislocations were presumably generated due to quenching stresses and were arranged in planar arrays.

Ageing of the solution treated samples in the temperature range of 923 K to 1223 K for various periods of time resulted in the precipitation of different intermetallic phases. The different precipitate species could be identified and distinguished from one another on the basis of the occurrence of reflections corresponding to them in selected area diffraction (SAD) patterns and also from their morphological characteristics. The general features of intermetallic phase precipitation were more or less similar to those reported by Paulonis et al. [3] and have been described in detail elsewhere [7–9]. Only some of these features will be dealt with in the present paper.

Precipitation of γ'' and γ' phases

Precipitates of the metastable γ'' and γ' phases formed in the alloy when ageing was carried out in the temperature range of 923 K to 1173 K for sufficient durations. SAD patterns obtained from suitably aged samples showed reflections corresponding to DO_{22} (γ'') and $L1_2$ (γ') structures. A typical [001] SAD pattern is shown in Fig. 4(a), in which precipitate reflections could be clearly observed at {100}, {110} and {1 1/2 0} positions. While reflections of the first two types could arise both from γ'' and γ' precipitates, those of the third type could be associated only with the γ'' phase. All these three types of reflections appeared in <001> SAD patterns obtained even from samples in which the precipitates were too small to be clearly resolved in dark field images. It appeared, therefore, that in this alloy γ' precipitation does not precede γ'' precipitation. It was not possible to test the alternative possibility, namely, whether γ'' precipitation precedes γ' precipitation, because of the difficulties in imaging extremely fine precipitates.

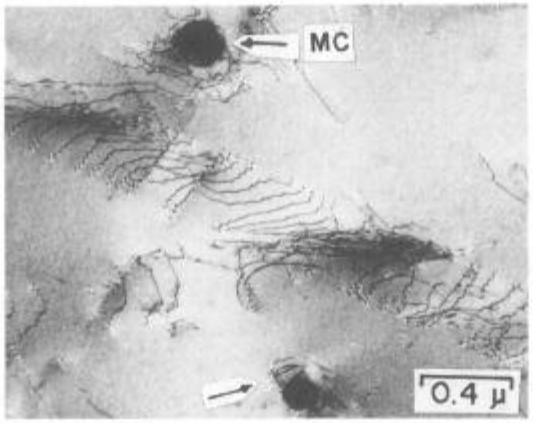

Fig. 3 - Primary carbide particles and planar arrangement of dislocations in a sample solution treated at 1373 K for 1 h and water quenched.

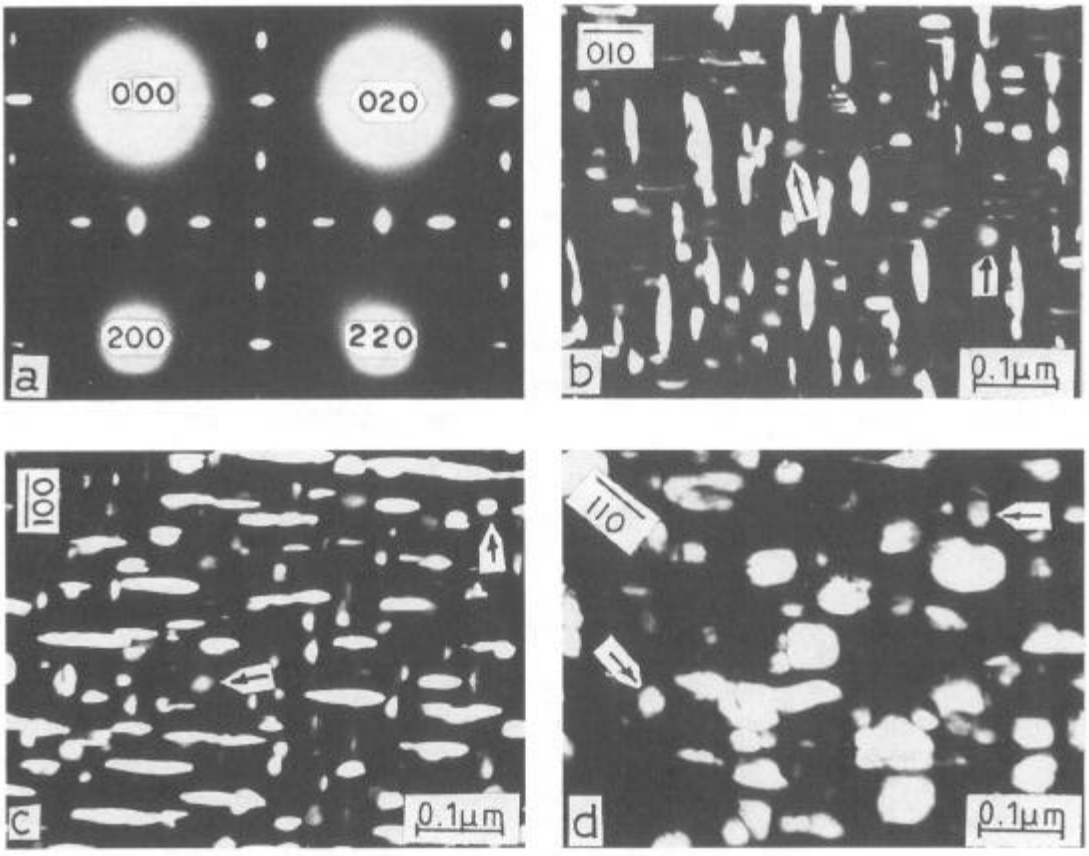

Fig. 4 - Typical microstructure of Inconel 718 aged at 973 K for 168 h. (a) [001] zone axis SAD pattern; (b), (c) and (d) show γ' particles (indicated by arrows) and different variants of γ" precipitates.

When the precipitates grew to larger sizes consequent to appropriate ageing treatments, particles of the two species could be distinguished on the basis of morphology. With the thin foil in a [001] orientation, two distinct precipitate morphologies could be observed in dark field images: some particles were nearly circular while some others were lens shaped. The former corresponded either to the γ' phase or to that γ'' variant for which the tetragonal axis was parallel to the electron beam. The latter corresponded to the other two γ'' variants. Those circular precipitates which could be imaged with {100} type as well as {110} type reflections belonged to the γ' phase; those showing up only under {110} type reflections corresponded to the γ'' phase. Some of these features are illustrated in Fig. 4(b) – (d). Precipitates of both the metastable phases were found to be homogeneously distributed in the matrix. The volume fractions of the γ'' and the γ' phases were approximately in the ratio 4:1 in the alloy used in this work. Even when the precipitates grew to quite large sizes they continued to remain coherent with the matrix. While the γ'' particles continued to be ellipsoidal, many of the γ' particles underwent a spheroidal to cuboidal shape change on prolonged ageing [9].

A frequent association between γ'' and γ' precipitates, leading to the appearance of certain composite morphologies, was noticed in samples aged for long periods in the temperature range of 973 K to 1023 K. The main features of the observed composite morphologies are enumerated below [9]. Illustrations are provided in Fig. 5.

(1) Some composite precipitates comprised a hemispherical γ' region with a plate–shaped γ'' region attached to the flat face of the hemisphere (Fig. 5 (a) – (b)). In some cases, the γ'' regions grew beyond the diameter of the hemisphere and produced a morphology consisting of a large γ'' disc attached to many small γ' precipitates (Fig. 5 (c)).

(2) Some near–cuboidal γ' particles were coated with γ'' particles on some of the cube faces (Fig. 5 (d) – (e)).

(3) γ' precipitates not associated with γ'' precipitates maintained a spherical shape even when they had grown to large sizes (Fig. 5 (f)).

(4) In some instances, γ'' precipitates appeared to be sandwiched between γ'regions (Fig. 5(g)) while in some others, the former were completely contained within the latter (Fig. 5 (h)). In some cases, γ'' precipitates appeared to impinge on and enter into γ' particles (Fig. 5 (i)).

(5) In some regions, γ'' precipitates belonging to two different variants appeared to intersect each other; the region of intersection appeared dark when imaged with superlattice reflections corresponding to either variant (Fig. 5 (j)–(k)). This contrast effect associated with the images of apparently intersecting γ'' precipitate variants could be explained by assuming that the precipitates were located one above other, along the foil thickness [18].

The coarsening kinetics of precipitates of both the species increased considerably when the ageing temperature was raised beyond 1023 K, leading to a reduction in the number densities of γ'' as well as γ' particles. Many large γ'' precipitates appeared to have faults within them (Fig. 6). These faults could be identified as stacking faults [6]. When the alloy was aged at 1173 K, the γ' phase did not precipitate though the γ'' phase did. This indicated that the γ' solvus in the alloy used was below this temperature.

Precipitation of δ phase

Ageing at 1023 K resulted in the precipitation of needle shaped δ precipitates at grain and

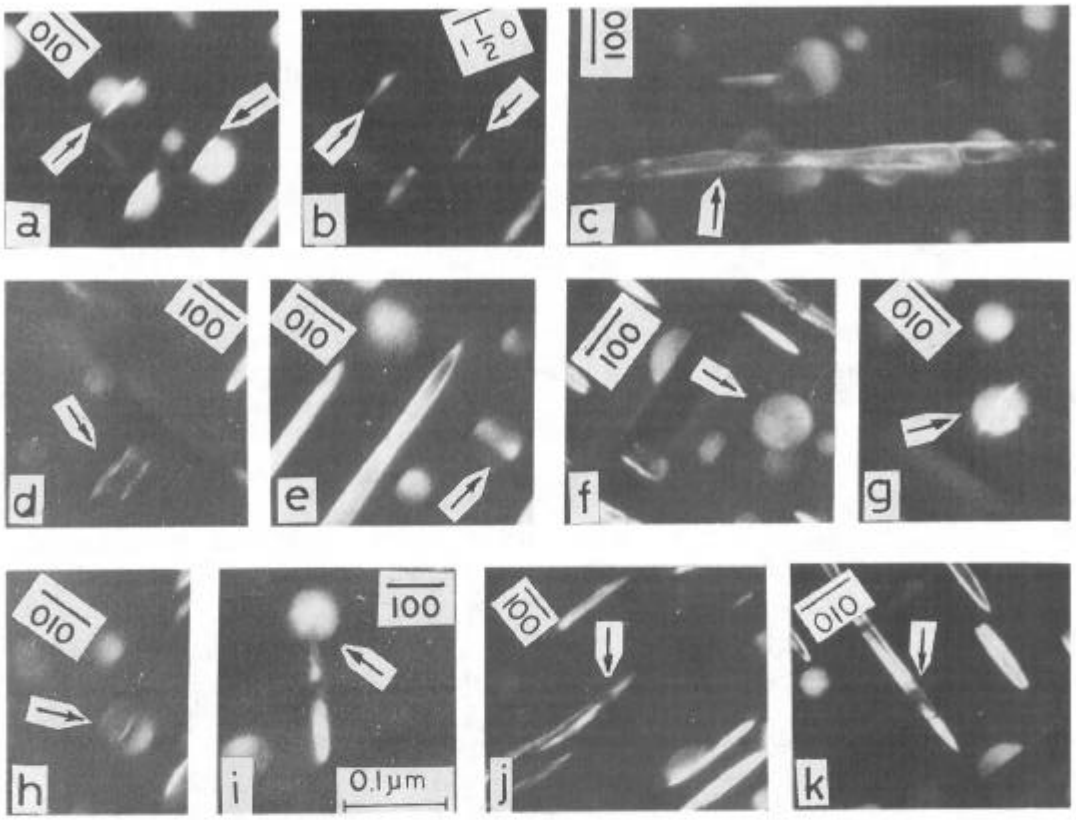

Fig. 5 – Typical dark field micrographs taken with electron beam direction along [001], illustrating the various type of association between γ" and γ' particles in Inconel 718 alloy aged at 1023 K. The g vector corresponding to the imaging reflection is marked in each micrograph. (a) and (b) are from the same region. Likewise, the pairs, (d) (e) and (j) (k) respectively are from two other specific regions. Regions of interest are marked by arrows (see text for details).

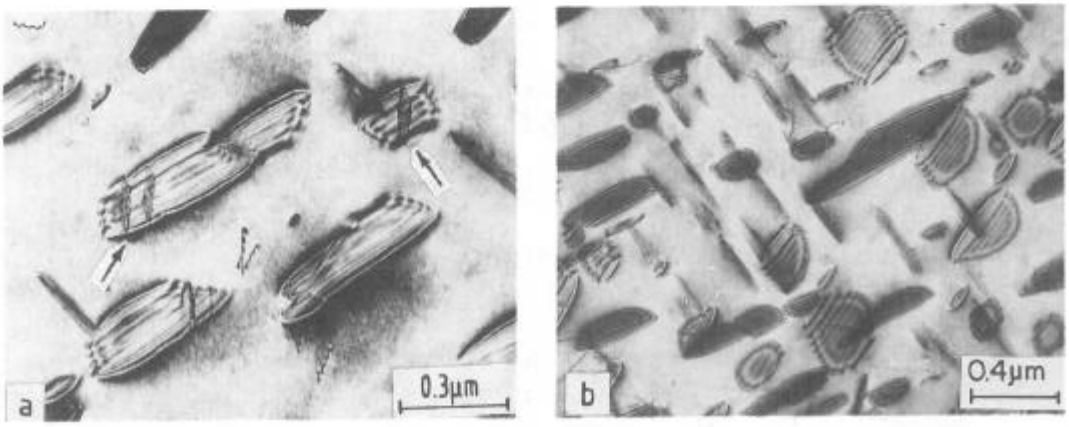

Fig. 6 – (a) Planar faults (marked by arrows) within large γ" particles, (b) Uniform distribution of γ" particles. Samples aged at 1173 K for 20 h.

twin boundaries (Fig. 7 (a)). Superlattice reflections in SAD patterns could be indexed in terms of the δ phase (Fig. 7 (b), (d)). The volume fraction of this phase increased with increasing ageing temperature and time. At the higher ageing temperatures δ precipitation occurred at intragranular sites also. Quite often δ precipitates were found to be surrounded by γ" precipitate free zones(PFZ), suggesting that the δ phase grew at the expense of the γ" phase (Fig. 7 (a), (c)). These zones, however, continued to be populated by γ' particles when ageing was carried out at temperatures below the γ' solvus temperature. Many large γ" precipitates contained stacking faults within them and these faults could be imaged in dark field with δ reflections (Fig. 8 (a)–(b)). This observation suggested that one possible mode of intragranular nucleation of the δ phase was in association with stacking faults within γ" precipitates. Dislocations, punched out during the growth of the δ particles to accommodate the misfit between the δ and the γ phases, were seen to interact with γ" precipitates, producing stacking faults within them.

At high ageing temperatures (e.g. 1173 K) the γ" precipitates were replaced by δ precipitates on prolonged ageing (Fig. 9 (a)–(b)). At 1223 K, the δ phase precipitated directly in the supersaturated matrix and the δ precipitates so formed exhibited both needle shaped and blocky morphologies [9]. From representative SAD patterns, the orientation relationship between the matrix and the δ phase was determined to be : $\{111\}_\gamma // (010)_\delta$; $<1\bar{1}0>_\gamma // [100]_\delta$, in conformity with that reported by Kirman [19]. The habit planes of the δ precipitates were determined by trace analysis to be the $\{111\}_\gamma$ planes. Four δ precipitate variants occurred in the austenite matrix.

Some of the observations made in this work on the precipitation of intermetallic phases in this alloy on ageing at different temperatures are summarised in Table II. As described earlier, the metastable γ' and γ" phases formed at lower ageing temperatures while the equilibrium δ phase precipitated at higher ageing temperatures. The temperature range over which the precipitation of the γ" and δ phases overlapped was quite wide in this alloy.

Flow behaviour

It has been observed that γ" precipitation strengthens Inconel 718 while the formation of the δ phase tends to bring down its strength [3,6]. In this work, the flow behaviour of the alloy at room temperature was studied as a function of the γ" precipitate size. The general nature of the flow curves appreared to be similar for solution treated and underaged specimens and showed a nearly linear dependence of the true stress on the true strain; by contrast a parabolic flow behaviour was exhibited by overaged samples [17]. The work hardening parameters were evaluated by following the Crussard and Jaoul formulation [20] in which the true flow stress, σ_t, is expressed as

$$\sigma_t = \sigma_0 + h\,\varepsilon_t^n$$

where ε_t represents the true plastic strain. The values of σ_0 (stress corresponding to $\varepsilon_t = 0$), the coefficient, h, and the strain hardening exponent, n, obtained from the experimental results pertaining to different heat treatments, are listed in Table III. It could be seen that the strain hardening exponent values could broadly be divided into two groups: one with $n \sim 0.85$ and the other with $n < 0.57$. The former corresponded to samples with average γ" precipitate radii smaller than about 10nm and the latter to those containing γ" particles of larger average radii. The values of the strain hardening exponent associated with solution treated and with underaged specimens were nearly the same although the corresponding yield strength values were very substantially different [17,21].

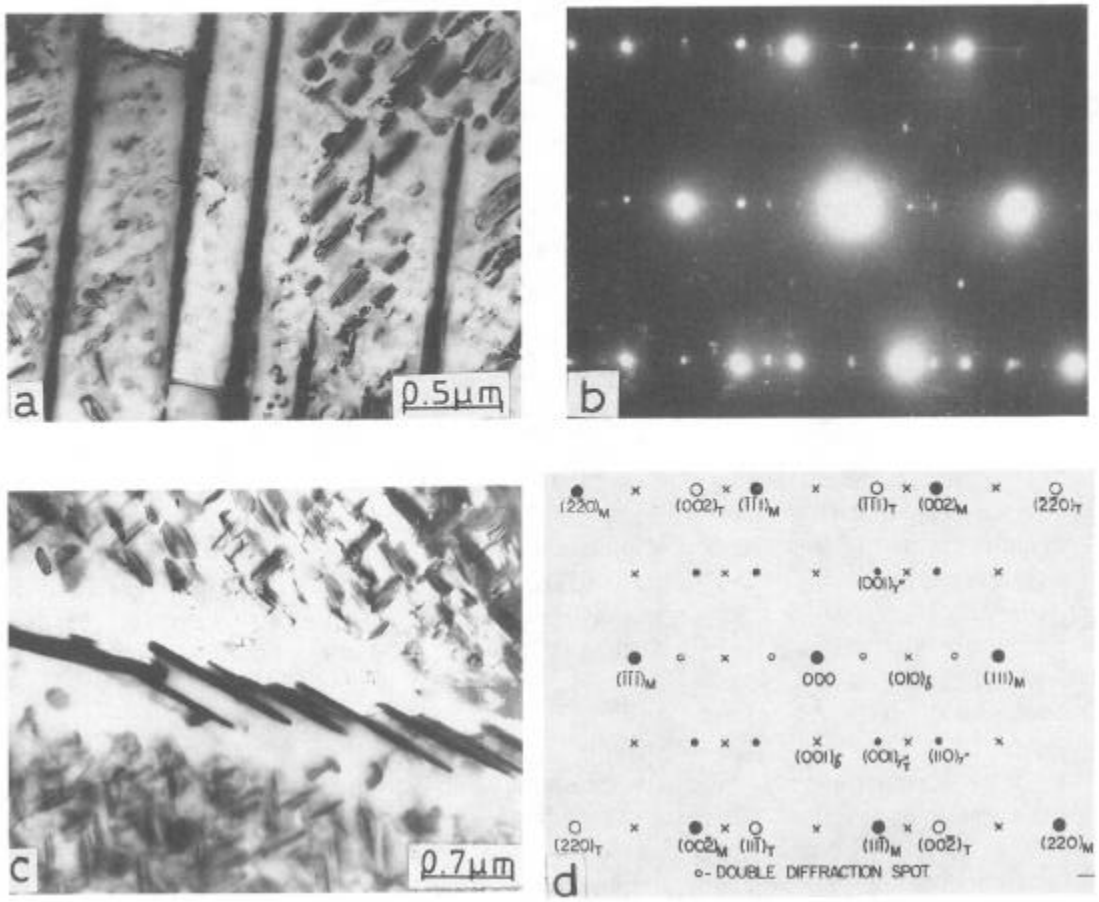

Fig. 7 – (a) Needle shaped δ particles at twin boundaries in Inconel 718 aged at 1023 K for 192 h; (b) SAD pattern corresponding to (a): (c) δ precipitation at a grain boundary (sample aged at 1073 K for 72 h); (d) Key to the SAD pattern in (b).

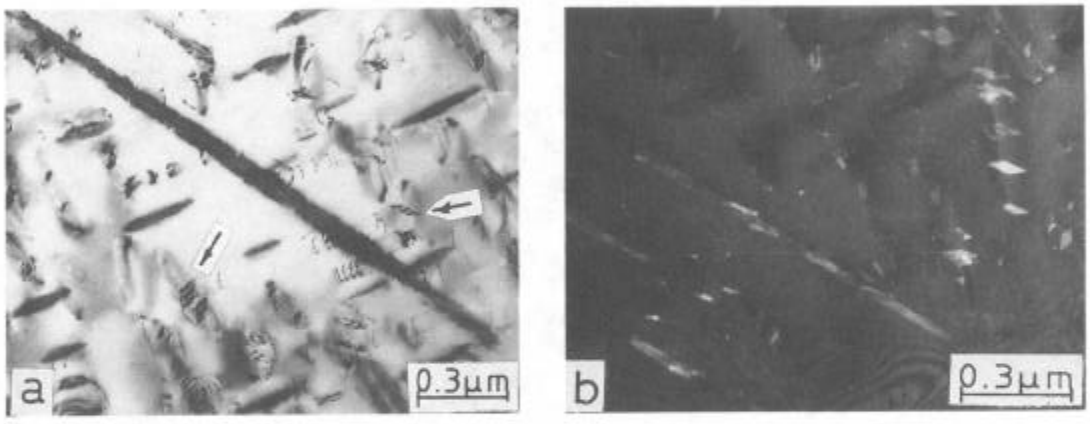

Fig. 8 – (a) Intragranularly nucleated δ precipitates in samples aged at 1073 K for 72 h. (b) δ precipitates and stacking faults within γ" precipitates imaged in dark field with $(\bar{1}10)_\delta$ reflection. Arrows in (a) indicate faults generated in γ" particles by dislocations punched out during the growth of δ precipitates.

Table II Observed Sequence of Intermetallic Phase Precipitation on Ageing Inconel 718 at different Temperatures.

γ (supersaturated) — $\gamma+\gamma'+\gamma''$	at 823 K < T < 937 K (even after prolonged ageing)
γ (supersaturated) — $\gamma+\gamma'+\gamma''$	at 973 K < T <1173 K (short time ageing)
γ (supersaturated) — $\gamma+\gamma'+\gamma''+\delta$	at 973 K < T <1173 K (prolonged ageing)
γ (Supersaturated) — $\gamma+\delta$	at 1173 K < T <1273 K

Table III Work Hardening Parameters and 0.2% Yield Strength (YS) as a Function of γ'' Particle Size.

Heat treatment	Particle size R (nm)	0.2% Y.S. σ(MPa)	Percentage elongation	σ_o (MPa)	h (MPa)	n
ST 1373 K–1h	–	280	63	298	1696	0.895
A973 K–1h	Unresolved	419	49	415	1734	0.804
A923 K–24h	2.0	641	36	650	1956	0.837
A973 K–8h	3.8	715	35	736	2015	0.822
A923 K–168h	10.0	985	15	915	1092	0.427
A973 K–24h	12.0	938	19	896	1432	0.532
A973 K–168h	28.0	820	18	581	1273	0.286
A1023 K–24h	35.0	580	25	610	1749	0.556
A1023 K–100h	60.0	490	23	604	1562	0.566

ST – Solution treated; A – Solution treated and aged.

Microstructure of the deformed alloy

The microstructural features of specimens deformed to small (eg., 2%) and large plastic strains are described briefly in the following.

Small deformation. The microstructure of solution treated samples revealed a planar arrangement of dislocations. These dislocations did not show any tendency for splitting into partials. Grouping of dislocations into pairs and less frequently, into quadruplets, was often noticed in specimens aged at 923 K for 24 hours and deformed to 2% strain (Fig. 10 (a)). These observations were in conformity with those reported earlier [16]. In samples containing large γ'' particles, only pairs of dislocations were observed [17]. Deformation induced faulting of γ'' precipitates was also noticed (Fig. 10 (b)).

Large deformation. The microstructure developed in samples subjected to large deformations was of two types, depending on whether the γ'' precipitates underwent deformation twinning or not. Deformation twinning was not observed in samples containing γ'' particles smaller than about 10 nm in radii; individual dislocations within deformation

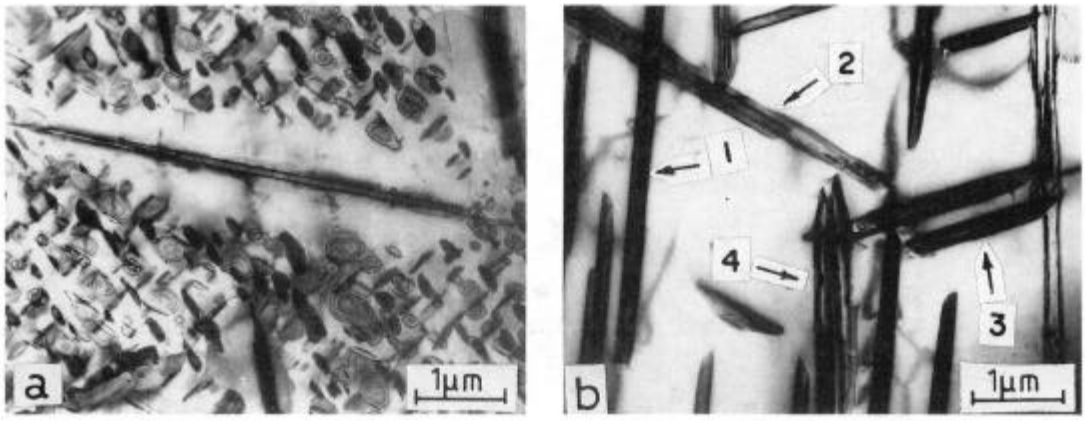

Fig. 9 – (a) γ'' free zones around δ precipitates. (b) Complete transformation to the δ phase. 1,2,3 and 4 denote different δ precipitate variants. Micrographs in (a) and (b) correspond to samples aged at 1173 K for 20 h and 100 h respectively.

bands could be resolved in many instances and twin reflections were absent in SAD patterns (Fig. 11 (a)). Profuse deformation twinning could be observed in specimens containing larger γ'' particles (Fig. 11 (b)–(d)). These precipitates appeared to have been fragmented into slices along the {111} planes. SAD patterns obtained from regions containing such precipitates showed streaking along the <111> directions in the reciprocal space and the extra spots along these streaks could be identified as twin reflections. Superlattice reflections corresponding to twinned segments of γ'' particles also appeared, e.g., the $(001)_{\gamma''}$ twin reflection midway between the (000) spot and the $(002)_T$ twin spot in $[1\bar{1}0]$ SAD patterns (Fig. 11 (d)). Such association of superlattice twin reflections with matrix twin reflections indicated that deformation twinning of γ'' precipitates conserved order within the twin bands and thus corresponded to a true crystallographic twinning. Dark field images obtained with $(002)_T$ twin reflection revealed that in some cases twins within γ'' particles propagated into the matrix as well. Serrated habit planes of γ'' precipitates belonging to the [001] variant were suggestive of fragmentation of these particles. The habit plane of this precipitate was found to be inclined to the $[001]_\gamma$ direction by about 13°, suggesting, that the offsets caused by deformation twinning led to a rotation of the average γ'' habit plane by about 13° with respect to the normal habit [17].

Thermal stability of deformation microstructure

Deformed samples containing γ'' particles with an average radius of about 28 nm were aged in the temperature range of 923 K to 1073 K for different periods of time. TEM examination of these aged samples showed that the deformation microstructure was stable upto 923 K. SAD patterns obtained from specimens aged at higher temperatures showed reflections corresponding to the δ phase in addition to those corresponding to the γ'' phase; dark field imaging revealed a uniform distribution of fine δ phase precipitates (Fig. 12 (a) – (b)). On increasing the ageing temperature, the intensity of δ reflections increased while that of γ'' reflections decreased and the δ precipitates grew in size (Fig. 12 (c)). The only intermetallic precipitate phase encountered in specimens aged at still higher temperatures (e.g. 1073 K) was the δ phase. However, intragranular δ precipitation was found to be absent in specimens subjected to identical ageing treatments but not to prior deformation.

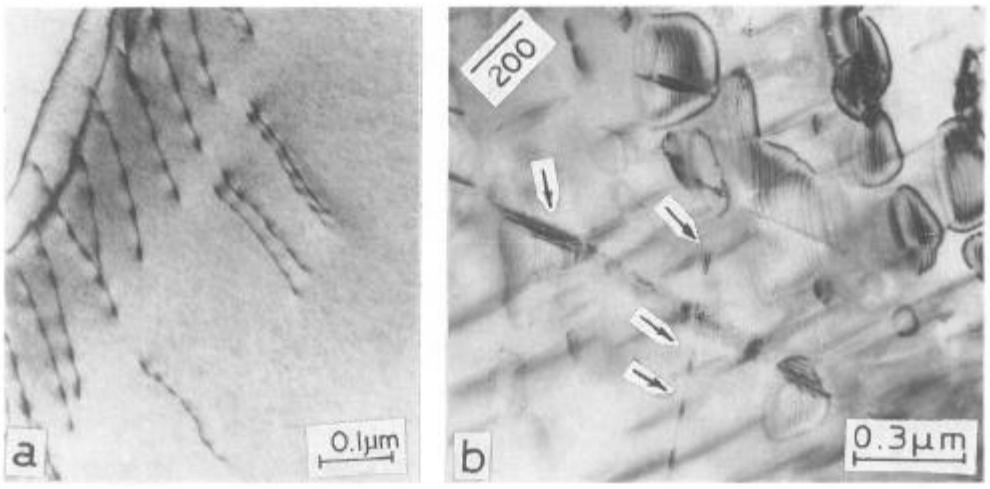

Fig. 10 – (a) Grouping of dislocations into quadruplets; (b) stacking faults (indicated by arrows) produced within γ" precipitates due to deformation; (a) and (b) correspond to samples aged at 923 K for 24 h and 1023 K for 130 h respectively and then deformed to 2% plastic strain.

Discussion

Some of the experimental observations described are discussed here.

Sequence of γ" and γ' precipitation

As mentioned earlier, it was possible to ascertain that γ' precipitation did not precede γ" precipitation in the alloy studied. However, it was not possible to determine whether both these phases precipitated more or less simultaneously or whether the γ" phase precipitated first. The observations made in this work indicated that the γ' phase was somewhat less stable than the γ" phase in this alloy in the sense that the former had a lower solvus temperature than the latter. Cozar and Pineau [15] have shown that the relative stabilities and volume fractions of these two metastable intermetallic phases in Inconel 718 type alloys are strongly influenced by the alloy composition, especially the ratio of the combined atomic concentration of titanium and aluminium to the atomic concentration of niobium. Their results have also shown that γ' precipitation precedes γ" precipitation in this class of alloys only when this concentration ratio is greater than about 0.8. Possibly this sequence of precipitation is not obtained in alloys for which this ratio is significantly smaller. It appears that such a situation prevailed in the case of the alloy used in this work, where the value of this ratio was only 0.66.

The effects of alloying elements on promoting or inhibiting the precipitation of different Ni_3X type phases in nickel base alloys can be qualitatively rationalised on the basis of the free electron concentration model and the s + p electron concentration model [22–24]. In the present discussion the precipitation of the different intermetallic phases in the alloy studied will be discussed in terms of the former. Of the three types of Ni_3X phases encountered in Inconel 718, the $L1_2$ (γ') and the DO_a (δ) structures are favoured when the electron concentration,e/a, (defined as the average number of electrons outside the inert gas shell per atom) value lies in the approximate ranges of 8.25 to 8.50 and 8.75 to 9.0 respectively [22].

In the DO_{22} and the DO_a structures, a rectangular arrangement of the minority atoms in the close packed planes is exhibited. By contrast, a triangular arrangement of the minority atoms in the close packed planes is obtained in the case of the $L1_2$ structure. On the basis of an examination of the stabilities of a large number of phases of A_3B stoichiometry, Sinha [22] has concluded that a transition from the triangular to the rectangular type of ordering on the close packed planes occurs when the e/a ratio attains a value of about 8.65. In the context of nickel base alloys, this value of the e/a may be considered to constitute the borderline between triangular ($L1_2$, γ') and rectangular (DO_{22}, γ'') intralayer ordering in metastable Ni_3X precipitate phases. The stoichiometric Ni_3Nb phase corresponds to a free electron concentration of 8.75. Partial substitution of elements such as iron and chromium for nickel and titanium and aluminium for niobium in Ni_3Nb in alloys like Inconel 718 would reduce the e/a ratio of this phase. Depending on the extent of substitution, the value of this parameter could thus be reduced from 8.75 to 8.65 and to still lower values. It appears that there is an upper limit for the electron concentration of Ni_3X phases with triangular layer ordering (e.g., γ') which is lower than the lower limit (8.65 electrons per atom) corresponding to Ni_3X

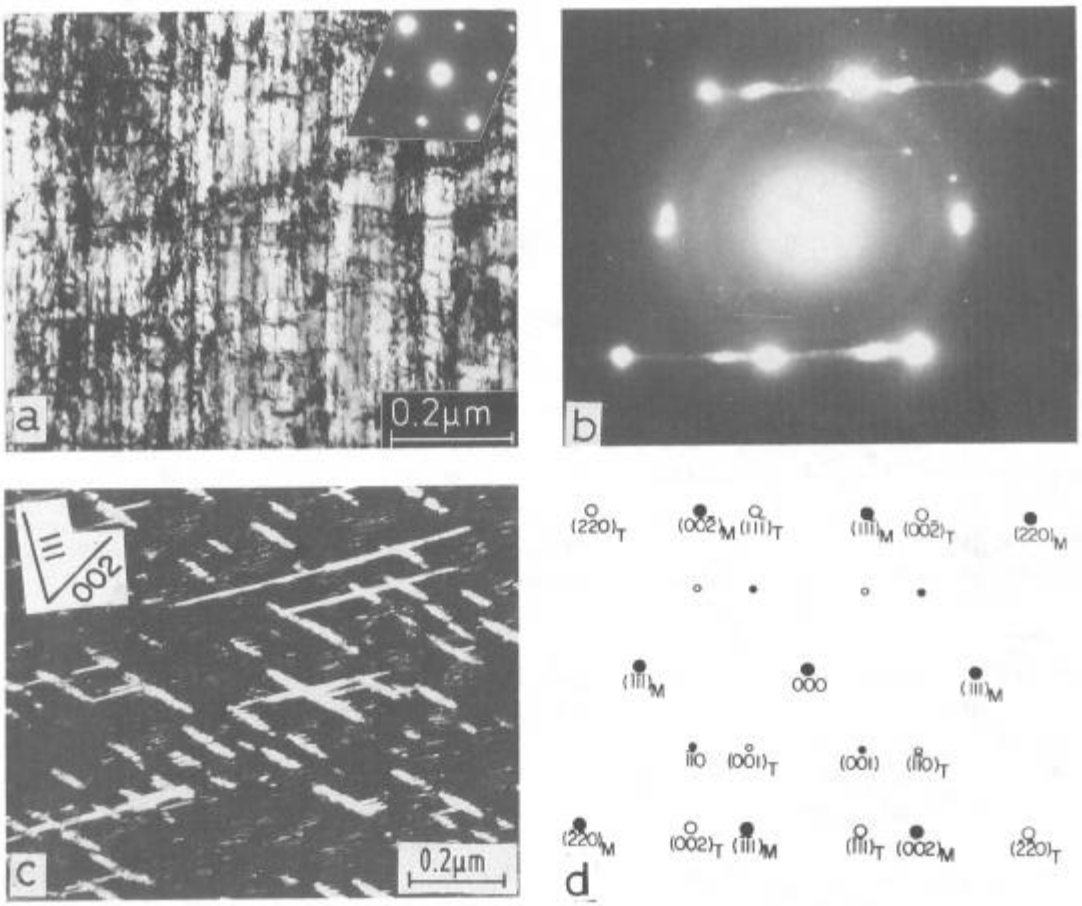

Fig. 11 –(a) Typical deformation microstructure observed in samples (aged at 973 K for 1 h) containing extremely fine γ'' particles and deformed to 48% plastic strain;(b)–(d) correspond to a sample aged at 973 K for 168 h and subsequently deformed to 2% cold work; (b) $[1\bar{1}0]$ SAD pattern showing superlattice twin reflection at $(001)_T$; (c) dark field micrograph with $g = (002)_T$ showing distribution of microtwins within different variants of γ'' precipitates on (111) plane; (d) Key to the SAD pattern in (b).

phases with rectangular layer ordering (e.g., γ") [22,25]. The simultaneous occurrence of γ' and γ" precipitates could, therefore, be expected in an alloy in which the alloying additions lower the e/a ratio to cause some γ' precipitation but are insufficient to bring down this parameter for all precipitates to levels below the limiting value for triangular layer ordering. The Inconel 718 alloy used in this work appeared to be an alloy of this type. The relative stabilities and the volume fractions of the two metastable intermetallic phases would be highly sensitive to changes in electron concentration brought about by alloy chemistry [9].

Composite γ'–γ" precipitate configurations

Although physical association between γ' and γ" precipitates was frequently observed, particularly in samples aged at 1023 K, the "compact morphology" described earlier was not observed in this alloy. The non–appearance of the "compact" morphology was consistent with the conclusion of Cozar and Pineau [15] that for this morphology to be exhibited the ratio of the total atomic concentration of titanium and aluminium to that of niobium should be greater than about 0.9. They have considered factors such as lattice parameter mismatches of γ, γ' and γ" phases and the effects of the concentrations of titanium, aluminium and niobium in the alloy on the incubation time for γ" nucleation following γ' nucleation for explaining composite precipitate morphologies. The lattice parameter of the γ' phase has a value intermediate between those of the lattice parameter of the γ and the 'a' parameter of the γ" phases; the interfacial energy requirements for γ" nucleation on a {100} face of a γ' precipitate would, therefore, be smaller than that associated with γ" nucleation in the austenite. Many examples of the nucleation of one metastable phase on another are known [26] and nucleation at matrix–precipitate interfaces has been rationalised by using heterogeneous nucleation theory [27]. However, if reduction in interfacial energy requirements were to be the sole factor responsible for the physical association between γ' and γ" precipitates, then one would expect the number of independently nucleated γ' or γ" particles, which did not show any physical association, to be very small. But a significant fraction of the γ' precipitates was of this type in the alloy studied. This was indicative of the simultaneous operation of some other mechanism also in respect of the evolution of the composite γ'–γ" morphologies. In this context, the "encounter mechanism" proposed by Davies et al. [28] appears to be very pertinent: two particles can join to form a composite single particle, during growth or coarsening, when their diffusion fields merge. Since solute elements like niobium, titanium and aluminium tended to partition to the γ" as well as the γ' phases in varying degrees [29] and since the number densities of both the precipitate species were quite high, it was possible that some of the composite γ'–γ" precipitate morphologies, examples of which are shown in Fig. 5, evolved through the joining of independently nucleated, neighbouring γ' and γ" particles. It was not possible to find out whether the observed physical association between the γ' and γ" precipitates was brought about by the nucleation of particles of one species on those of the other or by the merger and growth of independently nucleated precipitates of the two types. It was likely that both these mechanisms contributed to the formation of the composite γ'–γ" precipitate configurations [9].

Precipitation of metastable and equilibrium phases

On ageing the alloy at relatively low temperatures (below ~ 1173 K) the precipitation of the equilibrium δ phase was invariably preceded by that of the metastable γ" and γ' phases. At higher ageing temperatures, however, the δ phase precipitated directly from the supersaturated austenite matrix. In systems where metastable and equilibrium phases precipitate, the relation between the symmetry elements of the parent and the precipitate phases is a major factor in the selection of the path followed during the precipitation process. When the space group of the symmetry elements of a precipitate phase is a subgroup of the space group of the

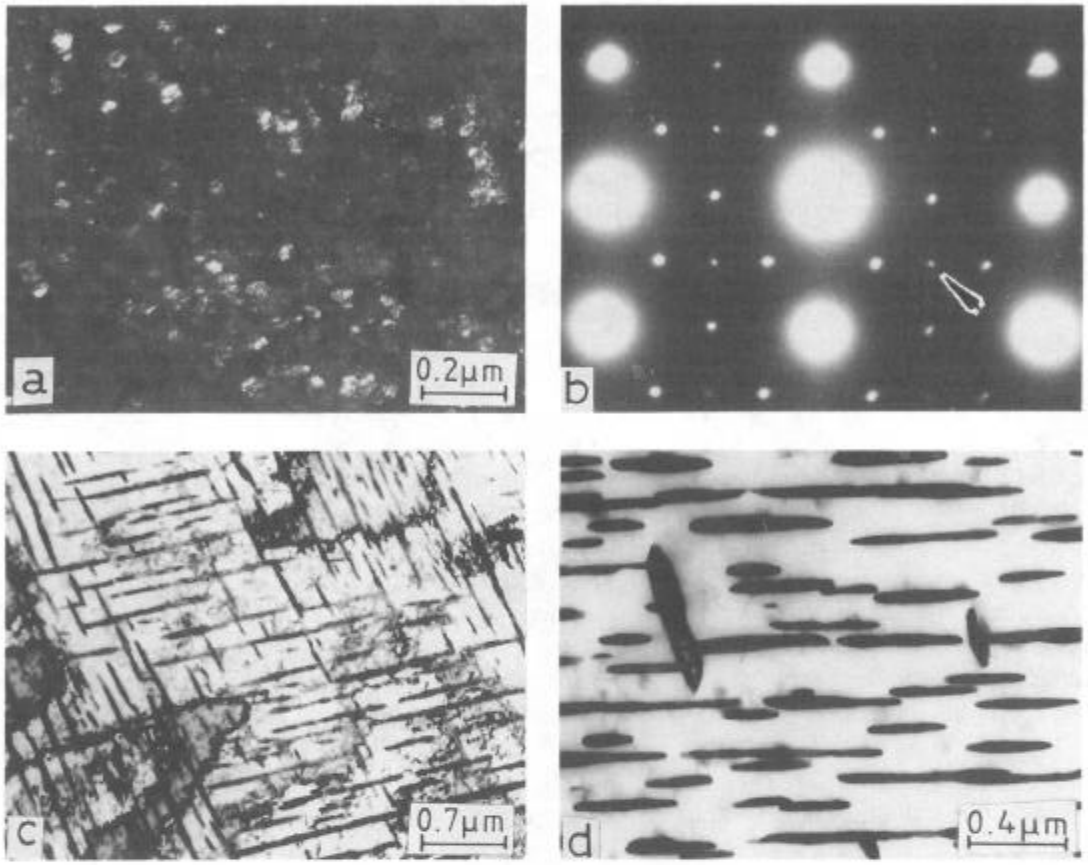

Fig. 12 – Micrographs in (a) (c) and (d) correspond to deformed samples subsequently aged at different temperatures. (a) Fine distribution of δ particles, mainly confined within γ" particles (aged at 973 K for 168 h); (b) SAD pattern corresponding to (a) showing δ reflections. (c) Accelerated growth of δ particles in samples aged at 1023 K for 168 h.(d) Complete replacement of γ" particles by δ particles in samples aged at 1073 K for 96 h.

symmetry elements of the parent phase, the formation of precipitates often involves replacement of atoms in the lattice positions of the matrix [30]. However, in situations where the precipitate phase is associated with some symmetry elements which are not present in the parent phase, the formation of precipitates cannot be brought about by a replacive ordering in the lattice of the matrix and precipitate nucleation involves the creation of a high energy interface. In the present case, the metastable γ' and γ" phases could both be generated from the parent γ phase (A1 structure) by replacive ordering. In such a situation, the matrix and the precipitate lattices can maintain coherency and the coherency strain depends on the difference in composition between the two phases. However, the formation of the δ phase, which is associated with an A3 (hcp) type stacking, could not occur by replacive ordering. The γ–γ' and the γ–γ" lattice mismatches were much smaller compared with the γ– δ lattice mismatch and obviously the nucleation barriers associated with the precipitation of the two metastable phases would be much smaller than that associated with that of the δ phase. It appeared that at low ageing temperatures the advantage of the high chemical free energy change, ΔG_v, associated with the formation of the δ phase, was offset by the much lower activation barriers associated with the nucleation of the γ" and γ' phases. However, at high ageing temperatures, close to the solvus of these metastable phases, the advantage of the low

non–chemical free energy requirement for the formation of the γ" and the γ' phases was nullified by the smaller ΔG_v values associated with the nucleation of these phases which were significantly lower than that associated with δ phase formation. At these temperatures, therefore, δ phase precipitation occurred directly from the solute supersaturated austenite phase.

γ" to δ transformation

As described earlier, essentially two modes of the precipitation of the δ phase were observed in the alloy studied: heterogeneous precipitation on grain and twin boundaries and intragranular precipitation, often in association with stacking faults located within pre–existing γ" precipitates [4,7]. Heterogeneous nucleation at structural singularities such as grain or twin boundaries is generally associated with a reduction in the activation barrier since the energy associated with the structural defect at which nucleation occurs can contribute to the minimisation of the non–chemical free energy requirement of the nucleation process.

The occurrence of stacking faults within γ" precipitates during their growth suggested that the stacking fault energy of this phase is low [9]. In fact, quite a few phases with the DO_{22} structure appear to have low stacking fault energies [31,32]. The nucleation of the δ phase on stacking faults within γ" precipitates can be explained in terms of the structures of these two phases. It has been pointed out earlier that the passage of an 1/6 $[11\bar{2}]$ partial on the (111) plane of a [001] γ" variant produces a geometric stacking fault without any first nearest neighbour violation. The formation of a stacking fault by the passage of such a partial on, say, the B_1 layer in the DO_{22} stacking sequence $A_1B_1C_1A_2B_2C_2$ $A_1B_1C_1A_2B_2C_2$.... would change the stacking sequence to $A_1B_1C_1A_2B_2C_2$ $A_1C_2A_1B_1C_1A_2B_2$ .. Thus the formation of a stacking fault on the B_1 layer would result in the creation of four successive layers ($C_2A_1C_2A_1$) with A3 (hcp) type stacking. As mentioned earlier, this type of two layer stacking is a characteristic of the crystal structure of the δ phase. Dark field imaging (e.g., Fig. 8(b)) demonstrated that the stacking faults within γ" particles did have a structure similar to that of the δ phase. These considerations suggested that δ nucleation often occurred by the growth of these faults into the matrix, forming laths that progressively grew to eventually replace the γ" precipitates [7].

Deformation of γ" precipitates

Quadruplets as well as pairs of perfect matrix dislocations glided through the γ" particles when their size was very small; at larger precipitate sizes, only dislocation pairs were observed [17,21]. This aspect will be discussed elsewhere. The observation of dislocation quadruplets and pairs would correspond to the movement of perfect unit dislocations whose passage through appropriate γ" precipitate variants restore order within them. In addition to shearing by groups of perfect dislocations, deformation of γ" particles by the passage of 1/6 <112> type partial dislocations also occurred. A perfect dislocation, on entering a precipitate, often split up into partials [17]. That partial whose passage would not change the first nearest neighbour bonds would glide through the γ" particle, creating a geometric stacking fault; the other partial, whose passage would lead to the formation of a complex stacking fault, would be stopped at the matrix–precipitate interface.

Deformation twinning

A noteworthy feature of the microstructure of heavily deformed specimens containing relatively coarse γ" precipitates was the profuse deformation twinning of these particles. The abundance of deformation twins within them testified to the fact that precipitate shearing could

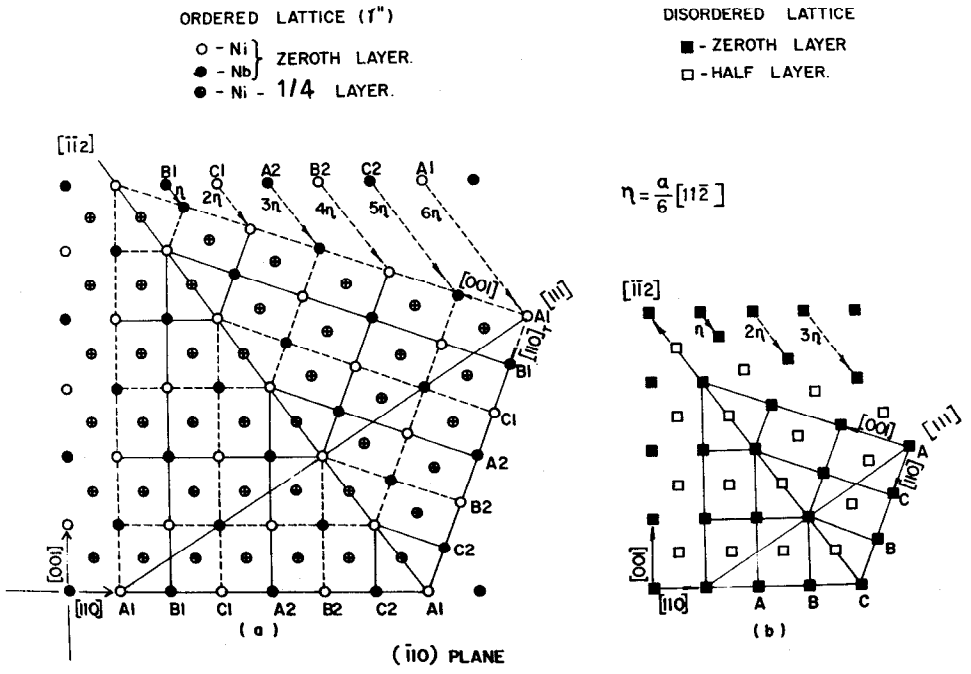

Fig. 13 – Schematic illustrations showing 1/6 [11$\bar{2}$] shear on every (111) plane resulting in a true crystallographic twins in the DO_{22} structure. (b) The same shear producing a twin in the A1 structure.

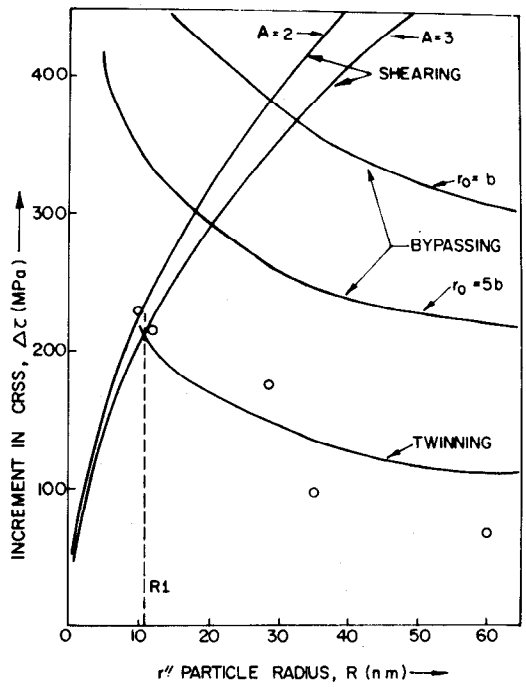

Fig. 14 – Calculated values of increment in shear stress, $\Delta\tau$, as a function of γ'' particle radius. Open circles represent experimentally determined values.

readily occur by deformation twinning. An analysis of the crystallography of twinning in the DO_{22} structure has been reported earlier and is illustrated in Fig. 13 [17]. The open and closed circles in Fig. 13 (a) represent nickel and niobium atoms respectively on the zeroth layer of the $(1\bar{1}0)_{\gamma''}$ plane while the crossed circles represent nickel atoms in the one fourth layer. The half layer and the three fourth layer, which contain nickel atoms only, coincide respectively with the zeroth and the one fourth layers. When a displacement of 1/6 $[11\bar{2}]$ is introduced on every (111) plane, a new orientation of the ordered DO_{22} crystal, which is twin related to the parent crystal, is generated. This is similar to the occurrence of {111} twinning in the A1 structure by the passage of a 1/6 $<11\bar{2}>$ partial dislocations on every {111} layer (illustrated in Fig. 13 (b)). It should be noted that in the case of the A1 structure the passage of any one of the 1/6 $<11\bar{2}>$ Shockley partials on every {111} plane would generate a twin orientation. In the DO_{22} structure, however, because of the ordered arrangement of atoms belonging to different species, shearing by only one specific Shockley partial in any specific {111} plane would lead to the formation of a twinned crystal. The preponderence of twins along different {111} planes has been attributed to Schmid factor values associated with each of the possible twinning mode for a given tensile direction [17]. The fact that a majority of the deformation twins were confined within γ'' the precipitates and did not propagate into the matrix suggested that the value of the critical resolved shear stress (CRSS) for twinning was higher in the austenite than in the γ'' phase.

Twinned γ'' to δ transformation

On ageing at temperature above 923 K, twinned regions of deformed γ'' particles transformed to the δ phase. The atomic layer stacking sequence across the γ'' – twinned γ'' interface, considering only the layers adjacent to the interface layer on either side and the interface layer itself, was $C_2A_1C_2$ (Fig. 13(a)). This stacking comprised the minimum number of layers necessary to generate the DO_a unit cell of the δ phase. Since the twinned γ'' regions had high energy interfaces with the matrix, nuclei of the δ phase initially grew at the expense of these regions (testified to by the disappearance of twinned γ'' reflections but not of γ'' reflections in SAD patterns), forming laths that eventually consumed the γ'' phase. The δ precipitates so formed during ageing of deformed specimens were very finely distributed in the matrix.

Effect of γ'' precipitate size on deformation mode

A slip to twin transition occurred in the mode of precipitate shearing as the γ'' particle size increased beyond a critical value of about 10 nm. The increments in the CRSS, $\Delta\tau$, associated with (i) slip by precipitate shearing and the passage of pairs of unit dislocations; (ii) slip by precipitate by passing with the formation of Orowan loops around γ'' particles, and (iii) deformation twinning of γ'' particles have been estimated as a function of the γ'' precipitate radii [17] and the plot is shown in Fig. 14. Experimentally observed values of shear stress increments are shown by open circles. Within the limits of experimental errors, these values were consistent with an $R^{-1/2}$ dependence of $\Delta\tau$, as predicted in the case of deformation twinning [17]. As mentioned earlier, no evidence of dislocation looping around γ'' particles could be obtained by TEM. The theoretically estimated critical γ'' precipitate size for the change in the deformation mode from slip to twinning agreed well with that experimentally observed. In a recent work the order strengthening in Inconel 718 in the presence of all the three γ'' precipitate variants has been estimated and it has been shown that the increase in CRSS, when all the three variants are present, is higher as compared to the case when only one variant of equivalent volume fraction is present [33]. In this treatment, it has been assumed that the γ'' particles are sheared by the movement of dislocation quadruplets. For the particle sizes at which the slip to twinning transition occurred, only dislocation pairs were

frequently observed and the calculations contained in Reference 17 were valid. One could also see from Fig. 14 that the CRSS required for deformation twinning in the γ'' precipitates would be smaller than that associated with Orowan bypassing for the entire range of precipitate sizes studied. A rough estimate of the stress required for twin nucleation (τ_T) in the γ'' phase gives a value of $\mu/\tau_T \sim 440$ where μ is the shear modulus of the matrix, assumed to be equal to that of the precipitate phase [17]. This value compares reasonably well with the experimentally determined values of the twin nucleation stress in some binary alloys and pure metals with the A1 structure [34, 35].

Work hardening behaviour

The room temperature work hardening behaviour of the alloy studied was interesting in the sense that the work hardening rate decreased as the γ'' precipitate radius increased beyond a value of about 10 nm. This observations indicated that precipitate bypass mechanisms did not operate when the γ'' particles were larger than this size and was consistent with the relevant TEM observations. Since the deformation twins were mostly confined within the γ'' particles, no grain partitioning by the deformation twinning of the matrix grains and the consequent increase in the work hardening rate [36] were not encountered. Since the stress required for the nucleation of deformation twins in γ'' particles was larger than that required for twin growth, the nucleation of twins would be followed by a "burst" of flow, resulting from the easy propagation of the twins across the precipitates; such microscopic bursts of easy flow did not cause the stress to drop but did bring down the work hardening rate in the alloy [17]. In the underaged alloy containing γ'' particles smaller than about 10 nm in radius, the passage of three or four pairs of dislocations or two groups of dislocation quadruplets could completely shear a precipitate into two separate halves. Once such a separation occurred, the trailing dislocations in the same slip plane would not see any ordered γ'' particles and their movement would resemble that of dislocations in the solution treated alloy [21]. For this reason, the work hardening rates were similar in the underaged and in the solution treated specimens.

Conclusions

On the basis of this work, the following conclusions could be drawn regarding the precipitation and the deformation behaviours of Inconel 718 alloy.

1. Precipitation of the γ' phase does not appear to precede that of the γ'' phase in this alloy.

2. Physical association between γ'' and γ' particles occurs quite frequently in a certain temperature range, giving rise to a variety of composite precipitate morphologies. However, the "compact" morphology does not appear to develop in an alloy of this composition.

3. Precipitation of the δ phase is preceded by that of the γ'' phase below $\sim$ 1173 K and at higher temperatures the δ phase precipitates directly from the austenite.

4. The δ structure can be generated by the introduction of geometric stacking faults in the γ'' structure. Experimental observations lend support to this contention based on lattice geometry.

5. At room temperature, the precipitate deformation mechanism changes form shearing to twinning (instead of looping) as the γ'' precipitate radius increases beyond a critical size of about 10nm. The flow stress required for deformation twinning of γ'' particles (for the particle size range studied in this investigation) is estimated to be smaller than that required for particle bypassing mechanisms to operate.

6. The change in precipitate deformation mechanism form shearing to deformation twinning is accompanied by a change in the strain hardening exponent form $\sim$ 0.8 to $\sim$ 0.5.

7. The deformation microstructure produced in the alloy by room temperature deformation is stable upto about 923 K. At higher temperatures profuse δ phase precipitation takes place.

Acknowledgements

The authors are indebted to Dr. C. K. Gupta, Director, Materials Group for constant encouragement and support.

References

1. D.R. Muzyka, in The superalloys, ed., C.T. Sims and N.C. Hagel (New York, NY: John Wiley, 1972), 113–143.
2. E.F. Bradley, ed., Source Book on Materials for Elevated Temperature Applications, (Ohio: ASM, 1979) 1–18
3. D.F. Paulonis, J.M. Oblak and D.S. Duvall, "Precipitation in Nickel Base Alloy 718", Trans. ASM., 62 (1969), 611–622.
4. I. Kirman and D.H. Warrington, "The Precipitation of Ni_3Nb Phases in a Ni–Fe–Cr–Nb Alloy", Metall. Trans., 1 (1970), 2667–2675.
5. Ya–fang Han, P. Deb and M.C. Chaturvedi, "Coarsening Behaviour of γ" and γ' Particles in Inconel 718 Alloy ", J. Metal Science, 16 (1982), 555–561.
6. M. Sundararaman, "Microstructural Studies on the High Temperature Materials Inconel 625 and Inconel 718 Alloys" (Ph.D. Thesis, Bombay University, 1986) 82–198.
7. M. Sundararaman, P. Mukhopadhyay and S. Banerjee, "Precipitation of the δ – Ni_3Nb Phase in Two Nickel Base Superalloys", Metall. Trans., 19A (1988), 453–465.
8. M. Sundararaman and P. Mukhopadhyay, "Intermetallic Phase Precipitation Behaviour of Two Wrought Nickel Base Superalloys", Metals, Materials and Processes, 3 (1991), 1–14.
9. M. Sundararaman, P. Mukhopadhyay and S. Banerjee, "Some Aspects of the Precipitation of Metastable Intermetallic phases in Inconel 718", Metall. Trans., 23A (1993), 2015–2028.
10. M.C. Chaturvedi and Ya – fang Han, "Strengthening Mechanisms in Inconel 718 Superalloy", J. Metal Science, 17 (1983), 145–149.
11. J.H. Moll, G.N. Maniar and D.R. Muzyka, "Heat Treatment of 706 Alloy for Optimum 1200°F Stres – Rupture Properties", Metall. Trans., 2 (1971), 2153 – 2160.
12. E.L. Raymond, "Effect of Grain Boundary Denudation of Gamma Prime on Notch Rupture Ductility of Inconel Nickel – Chromium Alloys X–750 and 718", Trans. TMS–AIME, 239 (1967), 1415–1422.
13. V. Ramaswamy, P.R. Swann and D.R.F. West, "Observations on Intermetallic Compound and Carbide Precipitation in Two Commercial Nickel–Base Superalloys", J. Less–Common Metals, 27 (1972), 17–26.
14. M. Sundararaman and P. Mukhopadhyay, "Carbide Precipitation in Inconel 718", High Temp. Materials and Processes, 11 (1993), 351–368.
15. R. Cozar and A. Pineau, "Morphology of γ" and γ' Precipitates and Thermal Stability of Inconel 718 type Alloys", Metall. Trans., 4 (1973), 47–59.
16. J.M. Oblak, D.S. Duvall and D.F. Paulonis, "Coherency Strengthening in Nickel Base Superalloys Hardened by DO_{22} γ" Precipitates", Metall. Trans., 5 (1974), 143–153.
17. M. Sundararaman, P. Mukhopadhyay and S. Banerjee, "Deformation Behaviour of γ" strengthened Inconel 718", Acta Metall., 36 (1988), 847–864.

18. M. Sundararaman and P. Mukhopadhyay, "Overlapping of γ" Precipitate Variants in Inconel 718", Materials Characterisation, 31 (1993), 191–196.
19. I. Kirman, "Precipitation in the Fe–Ni–Cr–Nb System", J.Iron and Steel Institute, 207 (1969), 1612.
20. C. Crussard and B. Jaoul, Rev. Metals, 57 (1950), 589.
21. M. Sundararaman, R. Kishore and P. Mukhopadhyay, "Strain Hardening in Underaged Inconel 718", Metall. Trans., 25A (1994), 653–655.
22. A.K. Sinha, "Close Packed Ordered AB_3 Structures in Ternary Alloys of Certain Transition Metals", Trans. TMS–AIME, 245 (1969), 911–917.
23. W.E. Quist, R. Taggart and D.H. Polonis, "The Influence of Iron and Aluminium on the Precipitation of Metastable Ni_3Nb Phases in the Ni–Nb system", Metall. Trans., 2 (1971), 825–832.
24. A.K. Jena, "On the Stability of Precipitating Phases in Nickel Base Superalloys", Materials Science Forum, 3 (1985), 281–289.
25. S.E. Axter and D.H. Polonis, "The Influence of Cobalt, Iron and Aluminium on the Precipitation of Metastable Phases in the Ni–Ta System", Mater. Sci. Engg., 60 (1983), 151–161.
26. K.C. Russell and H.I. Aaronson, "Sequences of Precipitate Nucleation", J. Mater. Sci., 10 (1975), 1991–1999.
27. P.E. Marth, H.I. Aaronson, G.W. Lorimer, T.L. Bartel and K.C. Russell, "Application of Heterogeneous Nucleation Theory to Precipitate Nucleation at G.P. Zones", Metall. Trans., 7A (1976), 1519–1528.
28. C.K.L. Davies, P. Nash and R.N. Stevens, "The effect of volume fraction on Ostwald Ripening", Acta Metall., 28 (1980), 179–189.
29. M.G. Burke and M.K. Miller, "Atom Probe Analysis of the Compositions of γ' and γ" Intermetallic Phases in Nickel Base Superalloy 718", Proc. M.R.S. Symposium on Alloy Phase Stability and Design, ed., E.P. Pope and A.F. Giamei (Pittsburgh, MRS, 1991),223–238
30. D.de Fontaine, "Configurational Thermodynamics of Solid Solutions", Solid State Physics, Vol.34 (1979), 73–272.
31. G. Vanderschaeve and B. Escaig, "Dissociation of ½ <112> Perfect Dislocations and Nature of Slip Dislocations in Ordered Ni_3V", J. De Physique–Lettres, 39 (1978), 74–77.
32. M. Khantha, V. Vitek and D.P. Pope, "An Atomistic Study of Dislocations and their Mobility in a Model DO_{22} Alloy", Mater.Sci. Engg., A152 (1992), 89–94.
33. M. Sundararaman, J.B. Singh and P. Mukhopadhyay, "Estimation of Order Strengthening in Inconel 718 type Alloys Containing All γ" Precipitate Variants", Scripta Metall. et Materialia, 29 (1993), 557–562.
34. J.A. Venables, in Deformation Twinning, ed., R.E. Reed – Hill, J.P. Hirth and H.C. Rogers, (New York, NY: Gordon and Breach, 1964), 77.
35. L. Remy and A. Pineau, "Twinning and Strain Induced F.C.C.– H.C.P. Transformation on the Mechanical Properties of Co–Ni–Cr–Mo Alloys", Mater. Sci. Engg., 26 (1976), 123–132.
36. A.M. Garde, E. Aigeltinger and R.E. Reed–Hill, "Relationship Between Deformation Twinning and the Stress–Strain Behaviour of Polycrystalline Titanium and Zirconium at 77 K", Metall. Trans., 4 (1973), 2461–2468.